J Intell Manuf (2011) 22:131–143
DOI 10.1007/s10845-009-0267-9

A neural network and multiple regression method for the characterization of the depth of weld penetration in laser welding based on acoustic signatures

Wei Huang · Radovan Kovacevic

Received: 7 February 2009 / Accepted: 27 April 2009 / Published online: 12 May 2009

Abstract The need for the control of the depth of weld penetration has been and remains of a long term interest in the automated welding process. In this study, the relationship between the depth of weld penetration and the acoustic signal acquired during the laser welding process of high strength steels is investigated. The acoustic signals are first preprocessed by the spectral subtraction noise reduction method and analyzed both in the time domain and frequency domain. Based on this analysis, two algorithms are developed to acquire the acoustic signatures. The acquired acoustic signatures are then used to characterize the depth of weld penetration by using a neural network and a multiple regression analysis. The results show that the acoustic signatures can characterize and predict the depth of weld penetration well under different laser welding parameters.

Keywords Acoustic signal · Depth of weld penetration · Neural network · Multiple regression

Introduction

Welding is the most frequently used method in the manufacturing industry to join metal components. As a main concern during the welding process, the depth of weld penetration is of great significance to the quality of as-welded structures. Due to a higher energy density, laser welding can achieve a deeper penetration at a higher welding speed compared to the traditional arc welding process; therefore, it is prevalent in the manufacturing industry as an effective and efficient method to join metal sheets. However, because laser welding is a highly complex process, multiple parameters such as the laser power, welding speed, material properties, protection gas, and joint set-up greatly influence the quality of the welds.

To detect the presence of weld defects and guarantee a high quality weld with the required depth of weld penetration achieved, different sensors and monitoring systems for laser welding are investigated and implemented in a number of researches. Among the different types of sensors, acoustic sensors draw much attention both from academia and industry. The acoustic sensors detect the pressure generated by the molten pool pulsation, plasma generation, thermal stress, metal vapor, and keyhole oscillation Sun and Elijah Kannatey-Asibu (1999). The signal transmitted through the material, which is called the acoustic emission (AE), has a frequency range from 50 to 900 kHz. The AE sensor is highly sensitive to interior events such as the formation of cracks, porosity and the phase transformation; however, the requirement that the transducer has to be in direct contact with the workpiece makes this type of sensor impractical in the industrial environment. In contrast, the acoustic sensor, which detects the sound pressure within the frequency range of 20 Hz to 20 kHz that is generated at the molten pool and transmitted through the air, does not have such a limitation. It is well known that an experienced welder can accurately judge the quality of the weld by listening to the sound produced during the welding process; therefore, airborne sound is extensively studied by a number of researchers. Shimada et al. (1982) used a microphone to study the weld penetration during laser welding and conclude that by measuring

W. Huang
Research Center for Advanced Manufacturing, Southern Methodist University SMU, 3101 Dyer Street, Dallas, TX 75205, USA
e-mail: huangw@smu.edu

R. Kovacevic (✉)
Department of Mechanical Engineering, Research Center for Advanced Manufacturing, Southern Methodist University SMU, 3101 Dyer Street, Dallas, TX 75205, USA
e-mail: kovacevi@smu.edu

the sound pressure level, the penetration state can be monitored. Gu and Duley (1996a,b,c) applied a frequency analysis and a statistical approach to the airborne sound signals acquired during the laser welding process. They investigated the effects of placing microphones at various locations on the accuracy of the acquired sound signals that reflect the quality of the welds. However, they found it difficult to identify the depth of weld penetration by monitoring the acoustic signal only. In addition to Gu and Duley's work, Farson et al. (1996) also investigated the acoustic signals produced during the laser welding of stainless steels and drew the conclusion that welds of poor quality can be differentiated from welds of good quality based on the acoustic energy in the frequency range of 1–2 kHz. Although the microphone is found to be useful to monitor the laser welding process, the obstacles posed by the noise that accompanies the acquired signal of interest and the highly complex relationship between the acoustic signal and the quality of the welds limits the broad application of microphones in the industrial environment.

To overcome the obstacles of using microphones to monitor the laser welding process, the objective of this study is to apply the proper digital signal processing methods to enhance the quality of the acoustic signal, and investigate the relationship between the acoustic signal and the depth of weld penetration. By applying a noise reduction method, the quality of the noisy acoustic signals acquired during the laser welding process of high strength steels is enhanced. The signatures of the acoustic signals are obtained by analyzing the acoustic signals both in the time and frequency domains. Based on the acoustic signatures, a neural network and a multiple regression analysis are used to establish a relationship between the acoustic signatures and the depth of weld penetration.

It is well known that the neural network has a powerful capability to perform nonlinear and multivariable mappings. Therefore, for the complex manufacturing processes, a neural network is always used to investigate the relationship between multiple inputs and outputs, to predict the outcome based on preset input parameters and to optimize the manufacturing processes. Mohanasundararaju et al. (2008) applied a neural network to predict the surface roughness in a grinding process for work rolls used in cold rolling. Kutschenreiter-Praszkiewicz (2008) adopted a neural network to determine the time consumption during a machining process so as to minimize the time and cost consumption. Wang et al. (2008) designed a neural-network based estimator to predict the tool wear during the hard turning process while Chao and Hwang (1997) adopted an improved neural network to predict the cutting tool life. Besides prediction and optimization, neural networks could also be used to fault detection and diagnosis (Kwak et al. 2000; Chumakov 2008). To characterize the complex relationship between the quality of the welds and the output signals of the sensor, a neural network is also frequently used. Park and Rhee (1999) adopted a neural network to estimate the bead size based on the optical signals acquired by three photodiodes in CO_2 laser welding. Saad et al. (2006) used a neural network based on acoustic signatures to distinguish the keyhole mode from the cutting mode in variable polarity plasma arc welding. While a neural network is an effective tool to map a complex relationship, a multiple regression analysis is a standard statistical technique used to establish the relationship between the independent and dependent variables, and it has the capability of predicting the dependent variable based on known independent variables. Park and Rhee (1999) also applied a multiple regression analysis to estimate the bead size in laser welding and made a comparison between the neural network and the multiple regression method. In this study, the depth of weld penetration is correlated to the acoustic signatures and welding parameters by applying a neural network and a multiple regression analysis. Based on the established relationship, the depth of weld penetration can be predicted by measuring the acoustic signatures. Consequently, an adaptive control for the depth of weld penetration can be achieved in the near future.

Experimental setup and results

Experimental setup

As shown in Fig. 1, the laser welding system consists of a 4-kW fiber laser with a welding head, a 6-axis robot, a venting fan, and a worktable. A free-field microphone is mounted beside the welding head. The distance between the microphone and the focal point of the laser beam is 22 cm, and the angle between the microphone and the worktable is 45°. The data acquisition (DAQ) system from National Instruments has a maximum sampling rate of 50 kHz, which can detect the audible acoustic signals in the frequency range of 20 Hz to 20 kHz. Two sheets of high-strength steel DP980 with a dimension of 200mm×40mm×1.5mm (length × width × thickness) are welded by a laser beam in a lap-joint configuration. The protection gas is argon with a flow rate of 30 SCFH, and the compressed air is used as the air-knife to

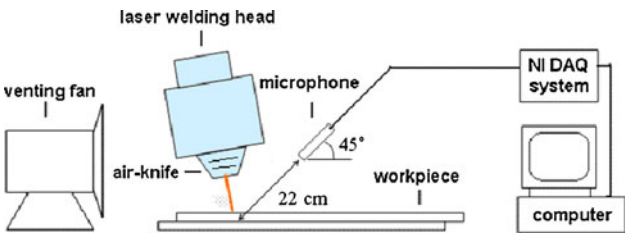

Fig. 1 Schematic diagram of the experimental setup

Table 1 Welding parameters in different experiments

Experiment index	Laser power (W)	Welding speed (mm/s)	Experiment index	Laser power (W)	Welding speed (mm/s)
1	2500	30	15	2500	50
2	2750	30	16	2750	50
3	3000	30	17	3000	50
4	3250	30	18	3250	50
5	3500	30	19	3500	50
6	3750	30	20	3750	50
7	4000	30	21	4000	50
8	2500	40	22	2500	60
9	2750	40	23	2750	60
10	3000	40	24	3000	60
11	3250	40	25	3250	60
12	3500	40	26	3500	60
13	3750	40	27	3750	60
14	4000	40	28	4000	60

protect the laser lens from spatters. A venting fan is placed beside the worktable to ventilate the vapor and fume produced by the laser-material interaction. The venting fan and the air-knife generate an intensive background noise during the laser welding process, which poses an obstacle for the acquisition of high-quality acoustic signals.

To investigate the relationship between the depth of weld penetration and the acoustic signals, 28 experiments with two repetitions of each experiment are performed under different welding parameters. The welding parameters adopted in these experiments are shown in Table 1. As the main factors that decide the heat input during the laser welding process, the laser power and welding speed are changed to achieve welds with different depths and accordingly the corresponding acoustic signals are acquired.

Experimental results

As shown in Fig. 2, the cross-sectional views of the 28 welds reflect the trend of how the depth of weld penetration changes under different welding parameters. When the laser power increases or the welding speed decreases, the depth of weld penetration increases. In order to establish the relationship between the depth of weld penetration and the corresponding acoustic signal, the depth of weld penetration is measured by an optical microscope, and the measured data are used later for a neural network and a multiple regression analysis.

Acoustic signal processing

Noise reduction

One of the objectives in this study is to apply proper digital signal processing methods to enhance the quality of the acquired acoustic signals. In the experimental environment of this study, the acoustic signals of interest are accompanied by a strong background noise from the air-knife and the venting fan. To minimize the effects caused by the background noise, a noise reduction method is chosen to remove the background noise from the contaminated acoustic signal of interest. The spectral subtraction method, a frequently used and easy-to-implement noise reduction method, is first proposed by Boll in (1979). The basic idea of the spectral subtraction method is to remove the background noise by estimating its spectrum when only the background noise is present, then subtracting this spectrum from the spectrum of the contaminated signal of interest. One assumption in applying the spectral subtraction method is that the spectrum of the background noise is relatively stable during the data acquisition process. This assumption is tenable in this study because the background noise produced by the air-knife and venting fan is stable during the welding process. This assumption can also be satisfied in an industrial environment as long as the combined spectrum of the complex noise signals is relatively stable.

In this study, as shown in Fig. 3a, the original noise signal produced by the air-knife and venting fan has a sound

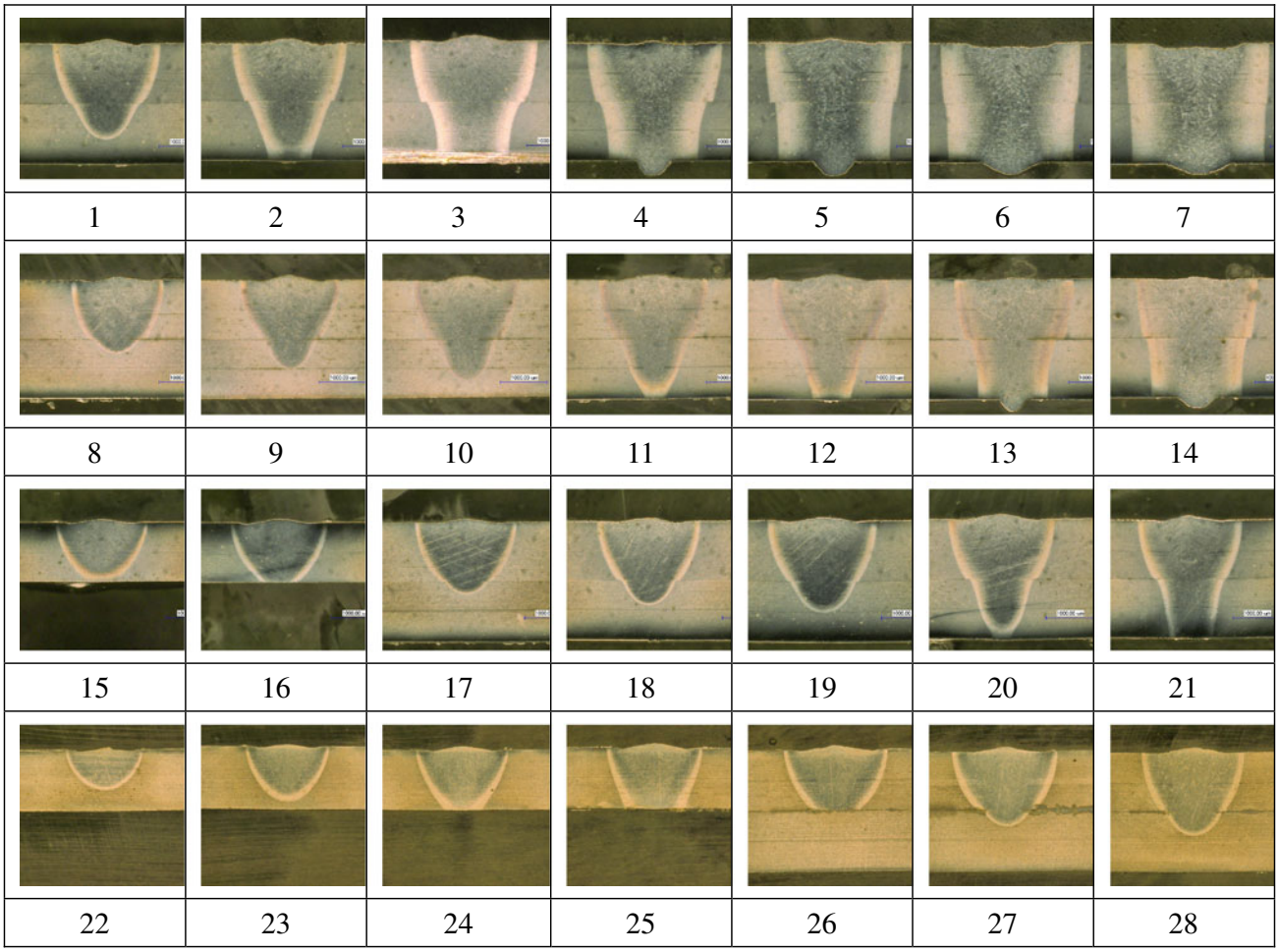

Fig. 2 Cross-sectional views of the welds under different welding parameters (4× magnified)

pressure level around 1 Pa. By applying the spectral subtraction to the background noise signal, the sound pressure level decreases to 0.05 Pa, as shown in Fig. 3b. From this comparison, it can be seen that the spectral subtraction greatly lowers the noise level, and consequently allows a high-quality signal of interest to be acquired for further signal analysis and acoustic signatures acquisition.

Signal analysis

During the 28 experiments carried out under different welding parameters, the corresponding acoustic signals are recorded in a sampling rate of 50 kHz. Before analyzing these signals in the time and frequency domains, the spectral subtraction is applied to these contaminated signals to maximally remove the background noise from the acoustic signals of interest. In order to extract the useful acoustic signatures from these 28 denoised signals, the signals acquired in experiments 1 and 5 are analyzed.

Analysis in the time domain

As shown in Fig. 4, the acoustic signals acquired in experiments 1 and 5 are first denoised by spectral subtraction. The welding parameters of experiments 1 and 5 are the same in the welding speed but different in the laser power. As shown in Fig. 2, a full weld penetration is achieved by a laser power of 3500 W (experiment 5) while only a partial weld penetration is achieved by a laser power of 2500 W (experiment 1). By observing the sound pressure level of the two different signals in the time domain, it is can also be noted that the signal from experiment 5 has a higher sound pressure level than that of the signal from experiment 1. This phenomenon indicates that the different depths of the weld produce different sound pressure levels of the acoustic signals, which result from the combined effects of the different pressures from the generated thermal stress, the plasma intensity, the molten pool pulsation and the oscillation behavior of keyhole between the different depths of weld penetration. This result is consistent with the conclusion made by Shimada et al.

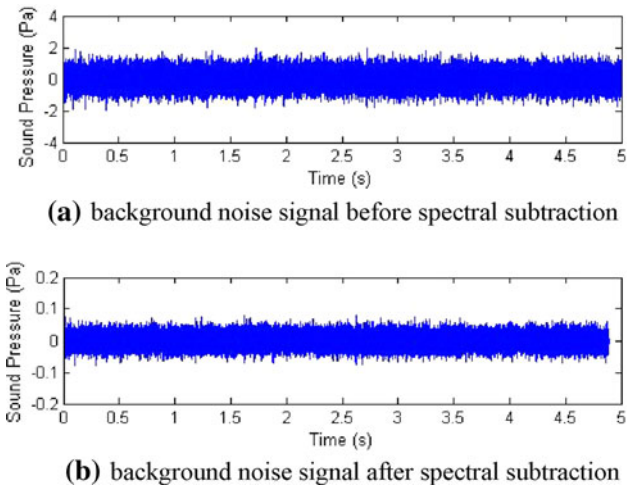

Fig. 3 Background noise signal processing

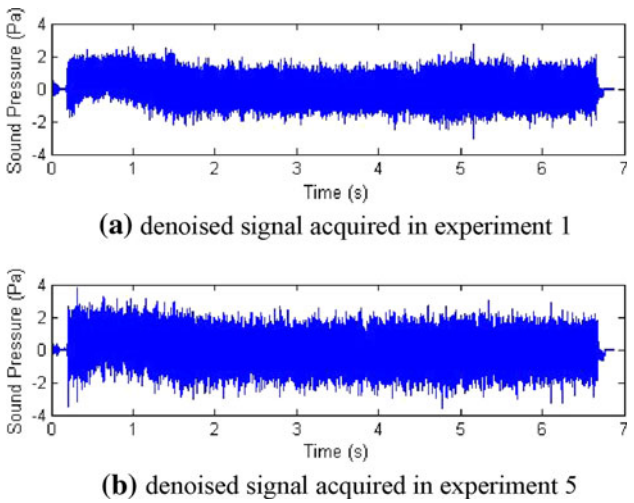

Fig. 4 Denoised acoustic signals from experiments 1 and 5 in the time domain

(1982) who reported that the penetration status can be monitored by measuring the sound pressure level of the acoustic signal during the laser welding process.

Analysis in the frequency domain

In addition to the analysis in the time domain, the two acoustic signals from experiments 1 and 5 are also analyzed in the frequency domain to acquire the different frequency characteristics of signals representing the different depths of weld penetration. According to Nyquist-Shannon sampling theorem, the frequency content from 0 Hz to 25 kHz of the signal can be obtained because the sampling rate in this study is 50 kHz. To investigate the audible acoustic signal, a frequency range from 0 Hz to 20 kHz is chosen for the signal analysis in the frequency domain. The measurement of the power spectrum density (PSD) of the acoustic signal is taken

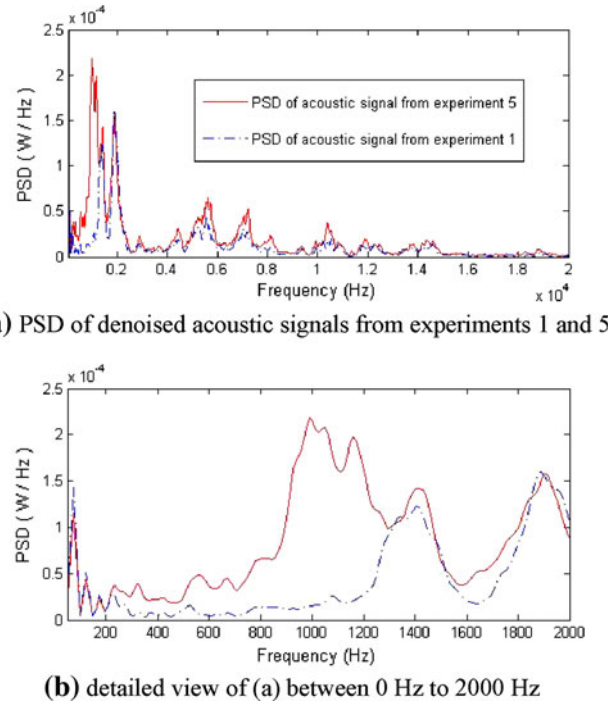

Fig. 5 Denoised acoustic signals from experiments 1 and 5 in the frequency domain

by applying the Welch–Bartlett method (Manolakis et al. 1999). This method estimates the power of the acoustic signal versus its frequency by averaging the individual periodogram thus reducing the variance of the individual PSD measurement, and results in a more accurate PSD estimate.

The results of the PSD analysis of the two signals from experiments 1 and 5 are shown in Fig. 5. It can be observed that the PSD of the two acoustic signals are different mainly in the frequency range from 500 to 1500 Hz. In other frequencies, the PSD of the two signals are almost the same. The detailed view of the different PSD distributions between 500 and 1500 Hz is shown in Fig. 5b. The dynamic behavior of the keyhole could be the cause for this difference in the PSDs of the two signals. As reported by Simon's research team (Kroos et al. 1993; Klein et al. 1994), the oscillation behavior of a keyhole has several eigenfrequencies that correlate to the physical and thermal properties of material. By investigating different materials, a conclusion was made that the typical frequency of keyhole oscillation behavior is around 1.5 kHz, and when the gas flow within the keyhole is not taken into consideration, the typical frequency of the keyhole oscillation is around 600 Hz. The difference in the PSD distributions of the acoustic signals from experiments 1 and 5 can be linked to the different intensities and sizes of the oscillation behavior of the keyhole in the frequency range of interest. It can be observed that in experiment 5 [see Fig. 2(5)], the keyhole is fully formed with a full penetration due to a higher laser power (3500 W), while in experiment 1 the keyhole is just

about to form, and the depth of weld penetration is much shallower due to the lower laser power of 2500 W.

Acoustic signatures acquisition

The same analyses as detailed above are applied to all 28 experiments, and the results show that the sound pressure level of the acoustic signal in the time domain and the PSD of acoustic signal in the frequency domain are closely correlated to the depth of weld penetration. In order to study the relationship between the acoustic signal and the depth of weld penetration, the acoustic signatures contained in the acoustic signal need to be extracted. To extract the acoustic signatures, algorithms are developed to perform the task. In the time domain, the difference in the sound pressure level can be calculated by the sound pressure deviation (SPD), which is the absolute difference between the sound pressure measured in each sampling point and the mean sound pressure of a set of sampling points. The algorithm in the time domain can be described in four steps as shown below:

(1) Divide the denoised signal X_n into small data sections $x_1, x_2, \ldots, x_m$ with an equal length of l. The length of the denoised signal is n. $m = n/l$.
(2) Calculate the mean values of sound pressure M_1, $M_2, \ldots,$ M_m for each data section: $M_i = \frac{1}{l}\sum_{k=1}^{l} x_{i(k)}$, $i = 1, 2, \ldots m$ and $k = 1, 2, \ldots, l$.
(3) Calculate the SPD at each sampling point for each data section: $SPD_{x_{i(k)}} = x_{i(k)} - M_i$.
(4) Integrate the sound pressure deviation for each data section: $SPD_i = \sum_{k=1}^{l} SPD_{x_{i(k)}}$.

In the frequency domain, a similar algorithm called band power (BP) can be also developed based on the different PSD distributions between the signals from the welds in different depths in the frequency band of [500:1500 Hz]. The algorithm can be carried out in three steps.

(1) Divide the denoised signal X_n to small data sections $x_1, x_2, \ldots, x_m$ with an equal length of l. The length of the denoised signal is n and $m = n/l$.
(2) Calculate the PSD of signals for each data section: $PSD_{x_i}(f) = P_{Welch\text{-}Bartlett}(x_i)$. $P_{Welch\text{-}Bartlett}$ is the calculated PSD of a signal over a frequency range of [0:$\frac{1}{2}$SR Hz]. SR is the sampling rate of the signal. $i = 1, 2, \ldots, m$.
(3) Integrate the PSD in the frequency band of [500:1500 Hz] for each data section to get the BP: $BP_i = \sum_{f=500}^{1500} PSD_{x_i}(f)$.

Because the main difference in the PSD distributions between the different signals lies in the frequency range from 500 to 1500 Hz, the 28 acoustic signals are first downsampled to 4000 Hz (SR = 4000). To guarantee the accuracy and resolution of calculating the SPD and BP of the acoustic signals, the two algorithms detailed above are applied to the 28 acoustic signals that have the same length of 12,000 sampling points (n = 12,000). This length corresponds to the acoustic signals acquired in 3 s, and the length of each data section is chosen to be 400 sampling points (l = 400). To investigate the relationship between the acoustic signatures (SPD and BP) and the welds at different depths, the mean values of the SPD_i and BP_i are used to establish this relationship. The acquired acoustic signatures (SPD and BP) are shown in Fig. 6. As shown in Fig. 2(1–14) and Fig. 6, by observing the trends of the depth of weld penetration and the SPD and BP when the welding speed is at 30 and 40 mm/s, it can be noted that before the full penetration is achieved, the SPD and BP almost linearly increase with the increase of the depth of weld penetration when the laser power increases. After the full penetration is achieved, in which case the depth of weld will not increase much further, the SPD and BP continue to increase when the laser power increases further. This is

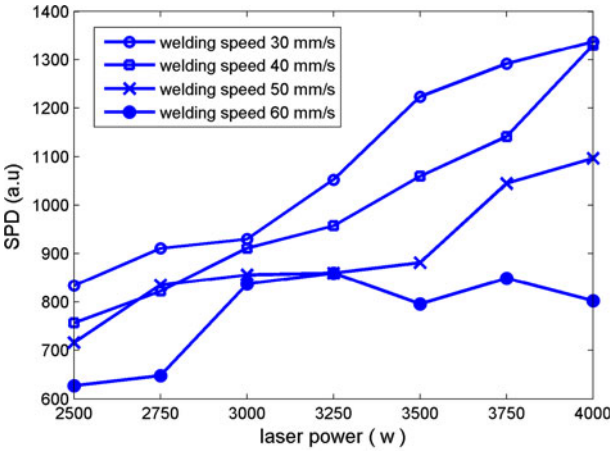

(a) SPD of 28 experiments

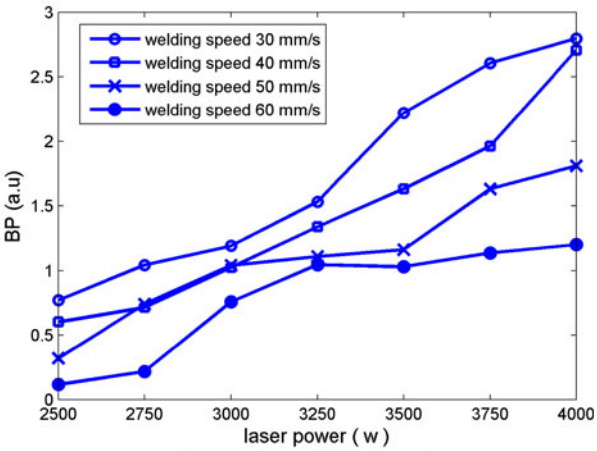

(b) BP of 28 experiments

Fig. 6 Acoustic signatures of 28 experiments

because when the laser continues to increase after the full penetration is achieved, a larger mass of metal is melted to form a wider molten pool and keyhole accompanied with more generated plasma and metal vapor, which consequently generate a higher SPD and BP. However, in the case when the welding speed is at 50 mm/s, the SPD and BP do not increase much when the laser power is increased from 2750 to 3500 W. This abnormality can be explained by observing the cross-sectional views of the welds as shown in Fig. 2(16–19). When the welding speed is at 50 mm/s and the laser power is lower than 3500 W, the depths of weld penetration are very shallow. In this so called heat conduction mode, where the keyhole is not formed, only a small mass of metal is melted and the mass of the melted metal increases slowly with the increase of the laser power. Consequently, the SPD and BP that reflect the pressure from the generated plasma, the molten pool pulsation, the metal vapor and the oscillation behavior of keyhole do not increase much with the slight increase of the depth of penetration. However, when the laser power is increased to 3750 W and higher, the depth of weld penetration, as well as the acoustic signatures SPD and BP, significantly increases. This increase in the depth of weld penetration and SPD and BP can be explained by the formed keyhole as shown in Fig. 2(20–21). In this so called keyhole mode, more heat input is absorbed by the workpiece due to the formed keyhole and therefore, more metal is melted and the depth of weld penetration is significantly increased at the transition phase of the keyhole. Meanwhile, the acoustic signatures SPD and BP are also much higher in this keyhole mode than that in the heat conduction mode because more plasma and metal vapor are generated and the oscillation behavior of the formed keyhole is much stronger. The same analysis can also be applied to explain the flat trends of the acoustic signatures SPD and BP when the welding speed is at 60 mm/s. When observing the cross-sectional views of the welds achieved when the welding speed is at 60 mm/s, as shown in Fig. 2(24–28), it can be noted that only heat conduction mode is present and no keyhole is formed when the laser power is between 3000 and 4000 W. Based on this observation, it can be concluded that the SPD and BP are closely related to the penetration mode and the depth of penetration. During the transition phase from the heat conduction mode to the keyhole mode, the depth of weld penetration greatly increases because more energy and heat input is absorbed by the keyhole and the acoustic signatures SPD and BP also significantly increase due to more generated plasma and metal vapor and a stronger oscillation behavior of the formed keyhole.

Characterization of the depth of weld penetration based on a neural network

In order to characterize the complex relationship between the acoustic signature and the depth of weld penetration, and predict the depth of weld penetration based on the acquired acoustic signatures, a neural network is adopted to perform this task. To successfully perform the task of establishing the mapping between the input variables and the output variables, there are four main issues that should be taken into consideration (Sukthomya and Tannock 2005).

- Input and output selection
- Training data collection
- Training and testing data preprocessing
- Network parameter selection

Inputs and outputs selection

To establish the mapping between the input and output variables, it is necessary to carefully select these variables. There are two methods to assign inputs and outputs to a neural network. The first method, which is called the global network, chooses all the available process parameters as the network inputs, and the network decides the weights of the process parameters by training itself. The training results of the global network emphasize the important input parameters by increasing their weights and ignore the insignificant input parameters by decreasing their weights. The second method, which is called the focused network, chooses those parameters that are considered to be more influential to the network outputs as the inputs. The focused network is always more efficient than the global one if no significant process parameters are missed (Wilcox and Wright 1998). In this study, as analyzed above, the main factors that influence the depth of weld penetration are the laser power and welding speed. Meanwhile, the two acoustic signatures (SPD and BP) also reflect the status of the depth of weld penetration. Therefore, the laser power, welding speed, and SPD and BP are selected to be the network inputs, and the depth of weld penetration is assigned as the network output.

Training data collection

To establish the mapping between the inputs and outputs, the neural network needs to be trained by the collected data. It is important to guarantee the integrity and sufficiency of the collected training data. Generally, there are three methods to collect training data. The first method is to collect data from some established models or simulations. The second method is to collect data from a real scenario, such as raw data from manufacturing companies. The third method is to collect data from designed experiments. The third method has advantages over the other two methods because it has more control over the data, and a wide range of data acquired from an optimally designed experiment can be obtained. In this study, as detailed in Table 1, the laser power and welding speed are

changed in a wide range to achieve different depths of the weld. The 28 experiments are carried out, and each of them is repeated once. In this way, the sufficient training data are collected to train the network. In addition to the network training, the network should also be tested by data that are unknown to the network. Those data are used to test the effectiveness of the network in establishing the mapping between the inputs and outputs. In this study, there are two ways to train and test the network. One way is to use the data from experiments 1, 2, 3, 4, 5, 6, 7, 22, 23, 24, 25, 26, 27, and 28 to train the network, and use data from experiments 8, 9, 10, 11, 12, 13, 14, 15, 16, 17, 18, 19, 20, and 21 to test the network. The other method is to use the data from odd numbered experiments 1, 3, 5, 7, 9, 11, 13, 15, 17, 19, 21, 23, 25, and 27 to train the network, and use the data from even numbered experiments 2, 4, 6, 8, 10, 12, 14, 16, 18, 20, 22, 24, 26, and 28 to test it.

Training and testing data preprocessing

The data should first be preprocessed by normalization before training and testing the network. The neural network can only perform well with data in certain ranges and in specified formats. If the data are out of the acceptable ranges for some transfer functions inside the network, the training results will be unreasonable. The other reason for data normalization is to ensure that each input parameter has the same contribution to the network training and testing processes. For example without normalization, the input with a range from 100 to 1000 may have a bigger effect on the output than another input with a range from 0.1 to 1. The normalization is important to the data acquired in this study because the four inputs have totally different ranges of data. The laser power varies from 2500 to 4000 W, and the welding speed varies from 30 to 60 mm/s. The SPD and BP also have different orders of magnitude; therefore, to normalize those input data into the same range can ensure the accuracy of the network. Among different normalization methods, the linear normalization is frequently used because it linearly transforms a data set from one data range to another without any distortion. In this study, the linear normalization is applied to the training and testing data sets, and all the data are normalized into the range of [0:1]. The equation for the linear normalization is described as follow:

$$x_{new} = \frac{x_{original} - x_{MinOR}}{x_{MaxOR} - x_{MinOR}} \quad (1)$$

where $x_{original}$ and x_{new} denote the data before normalization and after normalization. The x_{MaxOR} and x_{MinOR} denote the maximum and minimum values of the range of the original data set. For the four different inputs, the values of x_{MaxOR} and x_{MinOR} are given below, and the normalized training and testing data are shown in Table 2.

- SPD $x_{MaxOR} = 1400$ $x_{MinOR} = 600$
- BP $x_{MaxOR} = 3$ $x_{MinOR} = 0$
- laser power $x_{MaxOR} = 4000$ $x_{MinOR} = 2500$
- welding speed $x_{MaxOR} = 60$ $x_{MinOR} = 30$

Network parameters selection

After training and testing data are prepared for the neural network, the next step is to choose a proper structure for the neural network, and assign different parameters. Among those different structures, the multilayer feedforward neural network is the most commonly used because it is capable of approximating any nonlinear and multivariable mappings. However, determining the structure of this type of neural network is a difficult process since there is no general rule to guide this process. Therefore, the number of hidden layers and the number of the neurons at each hidden layer are usually decided by means of empirical testing. Usually, the number of hidden layers is not more than two layers because almost all the nonlinear relationships can be mapped by two hidden layers for a multilayer network. With regards to choosing a proper number of the neurons at each hidden layer, its objective is to minimize the errors between the predicted output and the actual output. If the number of the neurons is too small, the network can not learn the entire information well and will result in a big error. If the number of the neurons is too big, it will dramatically increase the computational cost and may result in over-train. Therefore, in this study, the number of neurons at the hidden layers is chosen to be 5, 10, 15 and 20 to train and test the neural networks in different structures. The trial-and-error method used in the training and testing process of the neural networks is to try different structures of the neural networks and calculate the errors between the predicted depth of penetration and the measured depth of penetration. Based on the statistical data of the mean and standard deviation of the error, the optimal structure of the neural network is decided. An example of the structure of a multilayer feedforward neural network that performs the mapping between the four input parameters and the depth of weld penetration is shown in Fig. 7. The transfer functions between the different layers are Log-Sigmoid functions that can map the inputs with an infinite range to the outputs within the range of [0:1]. In order to train the network, the back propagation algorithm is used. The basic idea of this training algorithm is to adapt the weights and biases of each neuron in the direction in which the performance function decreases most rapidly based on the error propagated backwards through the network. The performance function for the training of this network is the root mean square error (RMSE). In addition, the learning rate of the network is 0.05, the training epochs are 1000, and the goal of the RMSE for training is 1e-5. To investigate the effects of the network with

Table 2 Normalized data for NN and MR training and testing

Experiment index	Normalized SPD	Normalized BP	Normalized laser power	Normalized welding speed	Normalized depth of weld
1	0.2922	0.2565	0	0	0.6092
2	0.3887	0.3475	0.1667	0	0.7213
3	0.4125	0.3969	0.3333	0	0.8431
4	0.5657	0.5107	0.5	0	0.9477
5	0.7797	0.7403	0.6667	0	0.9544
6	0.8650	0.8684	0.8333	0	0.936
7	0.9216	0.9318	1	0	0.9322
8	0.1961	0.2005	0	0.3333	0.4245
9	0.2776	0.2381	0.1667	0.3333	0.5651
10	0.3893	0.3412	0.3333	0.3333	0.6586
11	0.4466	0.4458	0.5	0.3333	0.7368
12	0.5743	0.5437	0.6667	0.3333	0.8202
13	0.677	0.654	0.8333	0.3333	0.9462
14	0.9126	0.9022	1	0.3333	0.9171
15	0.1446	0.1066	0	0.6667	0.2483
16	0.2939	0.2467	0.1667	0.6667	0.3164
17	0.3202	0.3467	0.3333	0.6667	0.4055
18	0.3246	0.3693	0.5	0.6667	0.5097
19	0.3516	0.3872	0.6667	0.6667	0.5717
20	0.5557	0.5434	0.8333	0.6667	0.7592
21	0.6207	0.6029	1	0.6667	0.8204
22	0.0338	0.0389	0	1	0.1601
23	0.06	0.0725	0.1667	1	0.26
24	0.2964	0.2526	0.3333	1	0.3748
25	0.3248	0.3488	0.5	1	0.3952
26	0.2449	0.3432	0.6667	1	0.3965
27	0.3114	0.379	0.8333	1	0.5155
28	0.2529	0.4001	1	1	0.5842

a different number of hidden layers and neurons in each hidden layers, eight different structures are applied to train and test the neural network, and each of them performs the training and testing five times. As shown in Table 3 and 4, the results of the networks trained and tested by different data sets are given. The performances of the networks are evaluated by the mean value of the error rate (ER) and the standard deviation of the ER calculated for the testing data from 14 experiments. The ER is defined by Eq. 2.

$$ER_{(n)} = \frac{\left|x_{actual(n)} - x_{predict(n)}\right|}{x_{actual(n)}} \times 100\% \quad (2)$$

where $x_{actual(n)}$ is the measured value of the depth of weld penetration, $x_{predicted(n)}$ is the predicted value of the depth of weld penetration based on the trained network, and n is the experiment index used for network testing. The ERs shown in Table 3 and 4 are the mean values of $ER_{(n)}$.

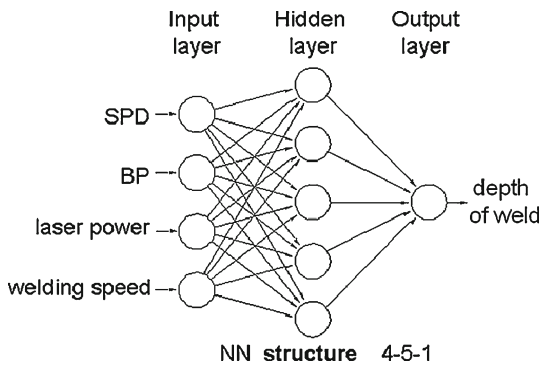

Fig. 7 Structure of a multilayer feedforward neural network

From the testing results, it can be observed that for networks (shown in Table 3) trained by the data from experiments 1, 2, 3, 4, 5, 6, 7, 22, 23, 24, 25, 26, 27, and 28, and tested by the data from experiments 8, 9, 10, 11, 12, 13, 14,

Table 3 Test results of NN

Experiment index for NN training: 1, 2, 3, 4, 5, 6, 7, 22, 23, 24, 25, 26, 27, 28

Experiment index for NN testing: 8, 9, 10, 11, 12, 13, 14, 15, 16, 17, 18, 19, 20, 21

NN index	Structure of NN	Mean of ER (%)	Std of ER (%)	NN index	Structure of NN	Mean of ER (%)	Std of ER (%)
1	4-5-1	21.81	21.07	21	4-5-5-1	17.95	12.14
2	4-5-1	19.77	20.14	22	4-5-5-1	18.88	27.07
3	4-5-1	22.72	19.90	23	4-5-5-1	18.80	16.26
4	4-5-1	16.64	14.32	24	4-5-5-1	13.48	10.88
5	4-5-1	15.84	18.67	25	4-5-5-1	11.25	12.59
6	4-10-1	14.75	12.95	26	4-5-10-1	22.96	22.63
7	4-10-1	18.47	16.92	27	4-5-10-1	19.35	19.42
8	4-10-1	26.52	17.89	28	4-5-10-1	10.33	11.97
9	4-10-1	16.07	15.32	29	4-5-10-1	17.70	17.01
10	4-10-1	19.91	17.70	30	4-5-10-1	16.05	9.78
11	4-15-1	12.25	12.72	31	4-5-15-1	12.09	10.36
12	4-15-1	17.25	10.62	32	4-5-15-1	16.03	12.23
13	4-15-1	15.22	10.46	33	4-5-15-1	18.27	11.40
14	4-15-1	14.21	9.55	34	4-5-15-1	14.45	11.73
15	4-15-1	16.89	17.35	35	4-5-15-1	19.22	16.09
16	4-20-1	12.96	8.85	36	4-5-20-1	15.56	9.10
17	4-20-1	13.70	11.56	37	4-5-20-1	17.42	14.23
18	4-20-1	9.97	6.78	38	4-5-20-1	21.99	13.54
19	4-20-1	15.81	11.33	39	4-5-20-1	13.83	24.62
20	4-20-1	15.70	10.03	40	4-5-20-1	12.23	8.25

4-5-5-1 means 4 input nodes at the input layer, 5 neurons at the first hidden layer, 5 neurons at the second hidden layer, and 1 output node at the output layer

15, 16, 17, 18, 19, 20, and 21, the mean values and standard deviations of the ER are mainly between 10% and 20%, which means the predicted depths of the weld are not consistent with the measured depths. These are unsatisfactory results for NN training and testing. In contrast, the networks (shown in Table 4) trained by the data from the odd-numbered experiments 1, 3, 5, 7, 9, 11, 13, 15, 17, 19, 21, 23, 25, and 27, and tested by the data from the even-numbered experiments 2, 4, 6, 8, 10, 12, 14, 16, 18, 20, 22, 24, 26, and 28 have better results because the mean values and standard deviations of ER are mainly smaller than 10%. The reason why the networks trained by different data sets have different results can be explained by the integrity of the data sets as required by the training data collection process. The training data set from the odd-numbered experiments 1, 3, 5, 7, 9, 11, 13, 15, 17, 19, 21, 23, 25, and 27 covers a full range of data acquired under different laser powers and welding speeds, while the other training data set from experiments 1, 2, 3, 4, 5, 6, 7, 22, 23, 24, 25, 26, 27, and 28 does not cover the data acquired under the welding speeds at 40 and 50 mm/s. Therefore, the networks as shown in Table 4 have better performances due to the integrity of their training data.

The best two networks trained and tested by different data sets are shown in Fig. 8. It can be observed that the depths of the weld achieved by the different welding parameters can be predicted well if the neural network has the proper structure and parameters, and if it is trained by an integral data set.

Characterization of the depth of weld penetration based on multiple regression

In addition to the neural network, a multiple regression analysis is also adopted to establish the relationship between the acoustic signatures and the depth of weld penetration. Multiple regression analysis is a statistical technique to predict the dependent variable on the basis of multiple independent variables. The dependent variable is modeled as a function of the multiple independent variables, corresponding coefficients, and errors to best fit the data. Usually, the best-fit criteria is evaluated by the minimum sum of squared errors (MSEE) that calculates the summation of the square of errors between the actual values of the dependent variable and the predicted values of the dependent variable from the estimated

Table 4 Test results of NN

Experiment index for NN training: 1, 3, 5, 7, 9, 11, 13, 15, 17, 19, 21, 23, 25, 27
Experiment index for NN testing: 2, 4, 6, 8, 10, 12, 14, 16, 18, 20, 22, 24, 26, 28

NN index	Structure of NN	Mean of ER (%)	Std of ER (%)	NN index	Structure of NN	Mean of ER (%)	Std of ER (%)
41	4-5-1	8.50	8.99	61	4-5-5-1	9.22	9.18
42	4-5-1	9.59	11.34	62	4-5-5-1	10.06	9.99
43	4-5-1	8.78	14.14	63	4-5-5-1	9.98	12.82
44	4-5-1	8.77	7.48	64	4-5-5-1	7.79	6.52
45	4-5-1	9.48	13.26	65	4-5-5-1	8.64	8.77
46	4-10-1	8.27	8.48	66	4-5-10-1	12.95	15.00
47	4-10-1	11.56	16.27	67	4-5-10-1	9.82	8.46
48	4-10-1	8.01	8.43	68	4-5-10-1	11.21	9.32
49	4-10-1	10.48	13.71	69	4-5-10-1	12.30	11.9
50	4-10-1	5.56	4.45	70	4-5-10-1	7.86	8.91
51	4-15-1	11.76	15.23	71	4-5-15-1	10.56	10.76
52	4-15-1	8.79	10.84	72	4-5-15-1	6.42	8.60
53	4-15-1	8.48	8.58	73	4-5-15-1	8.86	10.95
54	4-15-1	9.80	10.56	74	4-5-15-1	6.76	5.27
55	4-15-1	9.80	5.25	75	4-5-15-1	7.95	6.95
56	4-20-1	11.54	16.76	76	4-5-20-1	11.81	14.33
57	4-20-1	11.62	14.91	77	4-5-20-1	11.32	9.22
58	4-20-1	9.63	10.2	78	4-5-20-1	9.31	14.50
59	4-20-1	10.70	15.11	79	4-5-20-1	11.52	14.71
60	4-20-1	10.04	13.35	80	4-5-20-1	8.29	10.21

regression model. Commonly in regression analysis, the relationship between the dependent variables and the independent variables is first assumed to be a linear fashion. In this study, by observing the cross-sectional views of the welds in Fig. 2 and the trends of SPD and BP in Fig. 6, it can be observed that the relationship between the acoustic signatures, laser power, welding speed and the depth of weld penetration is indeed in a linear fashion. To quantitatively investigate if this assumption is tenable, the hypothesized relationship between the independent variables (SPD, BP, LP and WS) and dependent variable (DW) can be written as follows:

$$DW = \alpha + \beta_1 \times SPD + \beta_2 \times BP + \beta_3 \times LP + \beta_4 \times WS + \varepsilon \quad (3)$$

where DW is the depth of weld penetration, SPD is the sound pressure deviation, BP is the band power, LP is the laser power, WS is the welding speed, α is a constant, β_1, β_2, β_3, β_4 are the coefficients and ε is the "noise" term reflecting other factors that influence the depth of weld penetration. In this study, only SPD, BP, LP, and WS are considered to correlate to the depth of weld penetration, so the noise term ε is ignored here. The objectives of the regression analysis are to estimate the values of α and β_1, β_2, β_3, β_4 based on the training data set and test the model by examining the accuracy of the predicted DW on the basis of testing data set.

By applying the training data from experiments 1, 2, 3, 4, 5, 6, 7, 22, 23, 24, 25, 26, 27, and 28 to establish the model between the four independent variables and the depth of weld penetration, an equation describing MR model 1 is obtained, as shown in Eq. 4. To test the accuracy of the model, the data from experiments 8, 9, 10, 11, 12, 13, 14, 15, 16, 17, 18, 19, 20, and 21 are used to predict the depth of weld penetration. A comparison between the predicted depth of the weld by the MR model 1 and the actual depths of the weld are shown in Fig. 9a. As shown in Table 5, the mean value of the ERs between the predicted depth of the weld and the actual depth of the weld is *10.07%*, and the standard deviation of the ERs is*14.65%*. The same analysis method is applied to the MR model 2, which is trained by the data from experiments 1, 3, 5, 7, 9, 11, 13, 15, 17, 19, 21, 23, 25, and 27, and tested by the data from experiments 2, 4, 6, 8, 10, 12, 14, 16, 18, 20, 22, 24, 26, and 28. The MR model 2 is described by Eq. 5, and the comparison between the predicted depth of the weld and the actual depth of the weld is shown in Fig. 9b. The mean value of the ERs is *6.44%*, and the standard deviation of the ERs is *8.28%*.

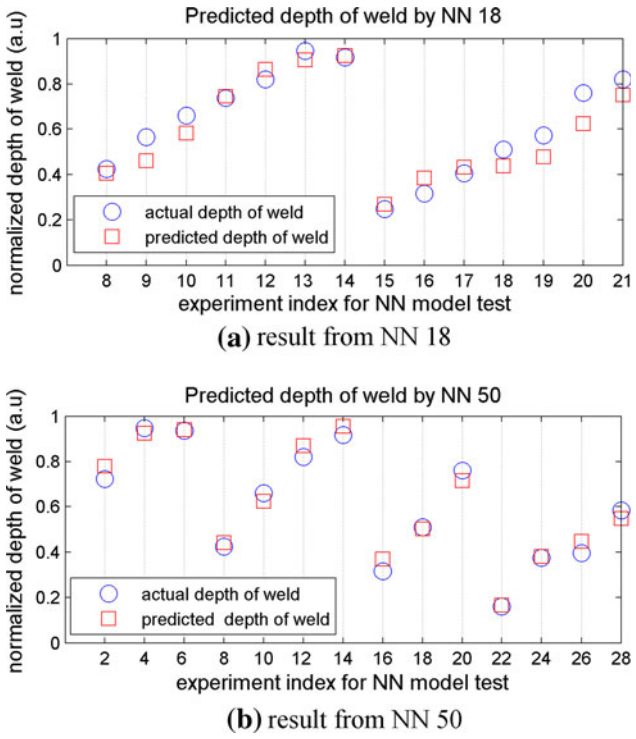

Fig. 8 Predicted depth of weld penetration by well-trained NNs

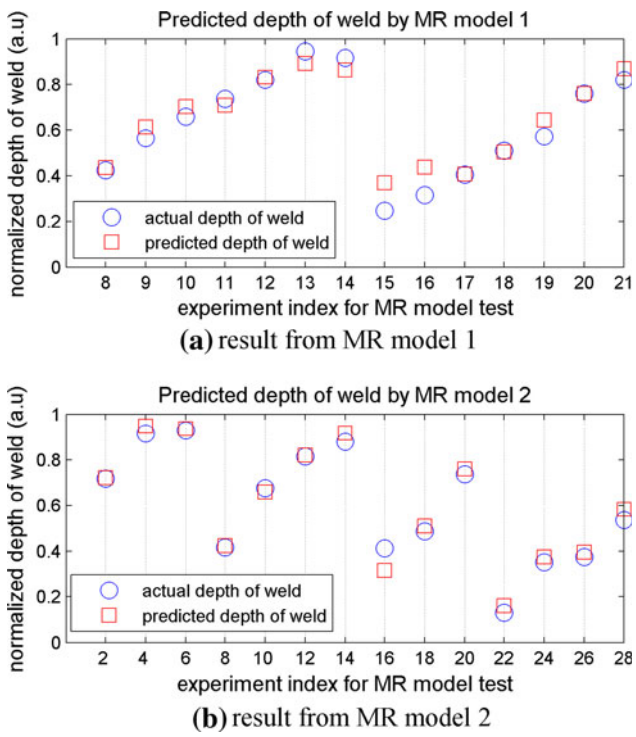

Fig. 9 Predicted depth of weld penetration by MR models

$$DW = 0.7428 + 1.4714 \times SPD - 2.0614 \times BP + 0.8227 \times LP - 0.5504 \times WS \quad (4)$$

$$DW = 0.6931 + 1.3376 \times SPD - 1.7893 \times BP + 0.7592 \times LP - 0.5387 \times WS \quad (5)$$

The models obtained by the multiple regression analysis, as shown in Eqs. 4 and 5, are linear in a four-dimensional space. By comparing the prediction results from the neural networks and the multiple regression models, it can be observed that for the neural networks 1–40 trained by the data from experiments 1, 2, 3, 4, 5, 6, 7, 22, 23, 24, 25, 26, 27 and tested by the data from experiments 8, 9, 10, 11, 12, 13, 14, 15, 16, 17, 18, 19, 20, and 21, the average mean value of ERs is *16.61%* and the average standard deviation of ERs is *14.39%*. For MR model 1, the corresponding mean value and standard deviation of ER are *10.07%* and *14.65%*, respectively. For the neural networks 41–80 trained by the data from experiments 1, 3, 5, 7, 9, 11, 13, 15, 17, 19, 21, 23, 25, and 27 and tested by the data from experiments 2, 4, 6, 8, 10, 12, 14, 16, 18, 20, 22, 24, 26, and 28, the average mean value of ERs is *9.60%* and the average standard deviation of ERs is *10.84%*. For MR model 2, the corresponding mean value and standard deviation of ER are *6.44%* and *8.28%*, respectively. From the comparison of the mean value and standard deviation of ERs, it can be concluded that the multiple regression models have a lower mean value of ERs and a lower standard deviation of ERs than the prediction results from the neural networks. This phenomenon indicates that the relationship between the acoustic signatures, the welding parameters, and the depth of weld penetration is more likely to occur in a linear relationship. The reason why the neural networks have a worse performance than the multiple regression models is because the neural networks with one or two hidden layers establish a nonlinear relationship between the inputs and outputs, resulting in inaccurate models. Therefore, when the structure of the neural network is selected to be 4-1, which means there is no hidden layer between the input layer and the output layer, the linear relationship, as described by Eqs. 4 and 5, as well as the prediction results, can also be obtained by the neural network in a structure of 4-1. This result illustrates that the relationship between the acoustic signatures, the welding parameters, and the depth of weld penetration is linear and the depth of weld penetration can be predicted well by the proposed models.

Conclusions

In this study, the acoustic signals acquired during the laser welding process of high strength steels are investigated to find a valid relationship between the acoustic signatures and the depth of weld penetration. By applying the noise reduction

Table 5 Test results of MR models

Experiment index for MR 1 training: 1, 2, 3, 4, 5, 6, 7, 22, 23, 24, 25, 26, 27, 28		
Experiment index for MR1 testing: 8, 9, 10, 11, 12, 13, 14, 15, 16, 17, 18, 19, 20, 21		
MR model 1	Mean of ER (%)	Std of ER (%)
$DW = 0.7428 + 1.4714 \times SPD - 2.0614 \times BP + 0.8227 \times LP - 0.5504 \times WS$	10.07	14.65
Experiment index for MR2 training: 1, 3, 5, 7, 9, 11, 13, 15, 17, 19, 21, 23, 25, 27		
Experiment index for MR2 testing: 2, 4, 6, 8, 10, 12, 14, 16, 18, 20, 22, 24, 26, 28		
MR model 2	Mean of ER (%)	Std of ER (%)
$DW = 0.6931 + 1.3376 \times SPD - 1.7893 \times BP + 0.7592 \times LP - 0.5387 \times WS$	6.44	8.28

method, the qualities of the acoustic signals are enhanced. Based on the analysis of these enhanced acoustic signals both in the time and frequency domains, the acoustic signatures such as the SPD and BP are extracted from the acoustic signals. The relationship between the acoustic signatures, the welding parameters, and the depth of weld penetration are investigated by the neural network and the multiple regression analysis. The results indicate that the relationship between the acoustic signatures, the welding parameters, and the depth of weld penetration is in a linear manner, and the depth of weld penetration can be predicted well by the proposed models.

Acknowledgements This work is financially supported by General Motors Corp and by the National Science Foundation, Grant No. EEC-0541952.

References

Boll, S. F. (1979). Suppression of acoustic noise in speech using spectral subtraction. *Acoustic, Speech, and Signal Processing, IEEE Transactions, 27*, 113–120.

Chao, P. Y., & Hwang, Y. D. (1997). An improved neural network model for the prediction of cutting tool life. *Journal of Intelligent Manufacturing, 8*, 107–115.

Chumakov, R. (2008). An artificial neural network for fault detection in the assembly of thread-forming screws. *Journal of Intelligent Manufacturing, 19*, 327–333.

Farson, D., Hillsley, K., Sames, J., & Young, R. (1996). Frequency-time characteristics of airborne signals from laser welds. *Journal of Laser Applications, 8*, 33–42.

Gu, H., & Duley, W. W. (1996a). Resonant acoustic emission during laser welding of metals. *Journal of Physics D: Applied Physics, 29*, 550–555.

Gu, H., & Duley, W. W. (1996b). A statistical approach to acoustic monitoring of laser welding. *Journal of Physics D: Applied Physics, 29*, 555–560.

Gu, H., & Duley, W. W. (1996c). Analysis of acoustic signals detected from different locations during laser beam welding of steel sheet. In *ICALEO* (pp. 40–48), Detroit, MI.

Klein, T., Vicanek, M., Kroos, J., Decker, I., & Simon, G. (1994). Oscillations of the keyhole in penetration laser beam welding. *Journal of Physics D: Applied Physics, 27*, 2023–2030.

Kroos, J., Gratzke, U., Vicanek, M., & Simon, G. (1993). Dynamic behavior of the keyhole in laser welding. *Journal of Physics D: Applied Physics, 26*, 481–486.

Kutschenreiter-Praszkiewicz, I. (2008). Application of artificial neural network for determination of standard time in machining. *Journal of Intelligent Manufacturing, 19*, 233–240.

Kwak, C., Ventura, J. A., & Tofang-Sazi, K. (2000). A neural network approach for detect identification and classification on leather fabric. *Journal of Intelligent Manufacturing, 11*, 485–499.

Manolakis, D. G., Ingle, V. K., & Kogon, S. M. (1999). *Statistical and adaptive signal processing* (pp. 227–232). Boston: McGraw-Hill.

Mohanasundararaju, N., Sivasubramanian, R., Gnanaguru, R., & Alagumurthy, N. (2008). A neural network and fuzzy-based methodology for the prediction of work roll surface roughness in a grinding process. *International Journal for Computational Methods in Engineering Science and Mechanics, 9*, 103–110.

Park, H., & Rhee, S. (1999). Estimation of weld bead size in CO_2 laser welding by using multiple regression and neural network. *Journal of Laser Application, 11*, 143–150.

Saad, E., Wang, H., & Kovacevic, R. (2006). Classification of molten pool modes in variable polarity plasma arc welding based on acoustic signatures. *Journal of Materials Processing Technology, 174*, 127–136.

Shimada, W., Ohmine, M., Hoshinouchi, S., & Kobayashi, M. (1982). A study on in-process assessment of joint efficiency in laser welding process. In *The fourth international symposium of the Japan Welding Society* (pp. 175–180), Osaka, Japan.

Sun, A., & Elijah Kannatey-Asibu, J. (1999). Sensor systems for real-time monitoring of laser weld quality. *Journal of Laser Applications, 11*, 153–168.

Sukthomya, W., & Tannock, J. (2005). The training of neural networks to model manufacturing processes. *Journal of Intelligent Manufacturing, 16*, 39–51.

Wang, X., Wang, W., Huang, Y., Nguyen, N., & Krishnakumar, K. (2008). Design of neural network-based estimator for tool wear modeling in hard turning. *Journal of Intelligent Manufacturing, 19*, 383–396.

Wilcox, J. A. D., & Wright, D. T. (1998). Towards pultrusion process optimization using artificial neural networks. *Journal of Materials Processing Technology, 83*, 131–141.